Analysis of Iron Losses on the Cutting Edges of Induction Motor Core Laminations

Paavo Rasilo, Ugur Aydin, Timo P. Holopainen, Antero Arkkio

***Abstract* – A 37 kW induction motor is modeled numerically taking into account the deterioration of the magnetic material properties at the cut edges of the core laminations. The magnetization properties and specific loss curves of the damaged edge and the intact material have been estimated from measurements published earlier. The deteriorated edges affect the iron losses of the machine in two distinct ways. First of all, the reduced permeability at the edges causes higher local flux densities elsewhere, which increases the losses. On the other hand, the cutting also has a direct effect on the specific loss density at the edges. By numerical simulations we show that the main effect is the latter one, and that the effect of decreased permeability remains low. The iron losses increase up to 37.6 %. The torque and active power of the machine are not much affected by the cutting, although also the current and resistive losses slightly increase due to the decreased permeability at the edges.**

***Index Terms*—Electrical machines, finite element analysis, magnetic materials, power losses.**

I. Introduction

THE MAGNETIC PROPERTIES of electrical steel sheets are known to be dependent on mechanical stresses and deformations, which occur especially when cutting the sheets. The core laminations of electrical machines are typically cut into the desired shape by punching. Laser cutting is often used for prototyping purposes when punching dies are not yet available. Rectangular samples e.g. for Epstein-frame measurements may be prepared with guillotine cutting. All of these cutting techniques deteriorate the magnetic permeability and increase the specific loss density near the cut edges of the sheets. This problem has been investigated quite comprehensively by experimental measurements [1]-[4]. Modeling attempts have also been made for estimating the effects of cutting on electrical machine cores [5]-[7].

In [5], the authors analyzed the effect of punching on the reluctance of a stator tooth of an airgapless prototype device both experimentally and numerically. The permeability was expressed as a function of the degree of plastic strain which was measured at different distances from a punched edge. A clear difference was observed in the flux-current relationships between non-annealed and annealed prototype devices. It was concluded that the whole 3 mm thick tooth is affected by the cutting.

In [6], two electrical machine stators were numerically modeled by expressing the permeability as a function of the distance from the cutting edge. The hysteresis losses were found to increase by 4.4-8.2 % due to the cutting, and it was estimated that due to the reduced permeability, the stator resistive losses would increase by 2-9 %. In [7], the authors estimated the mechanical stress distribution due to punching and calculated the effect of the punching on the iron loss. Drastic increases of 49 and 44 % were observed experimentally and numerically, respectively.

The modeling approaches of [5]-[7] only focused on the effects of cutting on the stator side of electrical machines. However, similar effects also occur on the rotor side if the rotors are stacked from laminations. Most of the rotor core losses in electrical machines occur very close to the air gap and thus very close to the cutting edges. Therefore it is of interest to quantify the effects of cutting also on the rotor side. In addition, the earlier comparisons were performed at constant current supply, and the actual reasons behind the iron-loss increases were not very carefully discussed. In fact, the deterioration of the magnetic properties at the cutting edges affects the iron loss in two distinct ways. First of all, in voltage-supplied machines, the reduced permeability at the cutting edges causes higher local flux densities elsewhere, which already increases the losses. In addition, the cutting also has a direct effect on the specific loss density curves at the edge. In this paper, we present a comprehensive numerical analysis of the aforementioned iron loss mechanisms in an induction motor.

We take advantage of the results of [1], in which the effect of cutting on the magnetic properties of rectangular non-oriented electrical steel-sheet samples was studied by measuring the magnetization and specific loss-density curves as a function of the cutting length per mass of the sample. In another ICEM 2016 submission [8], we describe a method for estimating the magnetization properties and specific loss densities both on the cutting edges and the intact part of the sheets measured in [1]. We found that the measurement results can be accurately reproduced by an analytical model in which the magnetization and power-loss properties are deteriorated in a 1.69 mm wide region near the edges. In this paper, we apply the results of [8] in a comprehensive numerical investigation on how the deteriorated material properties affect the performance of a 37 kW induction motor. The machine is modeled with the 2-D finite element (FE) method in which the deteriorated material properties are applied at the finely-discretized edge layer. By accounting for the deteriorated magnetization properties and the specific loss density curves in separate simulations, we are able to quantify in which proportion the two phenomena affect the performance of the machine. The

P. Rasilo acknowledges the Academy of Finland for financial support. The research leading to these results has received funding from the European Research Council under the European Union's Seventh Framework Programme (FP7/2007-2013) / ERC grant agreement n°339380.

P. Rasilo is with the Department of Electrical Engineering, Tampere University of Technology, Tampere, Finland and also with the Department of Electrical Engineering and Automation, Aalto University School of Electrical Engineering, Espoo, Finland (e-mail: paavo.rasilo@tut.fi).

U. Aydin and A. Arkkio are with the Department of Electrical Engineering and Automation, Aalto University School of Electrical Engineering, Espoo, Finland (e-mails: ugur.aydin@aalto.fi, antero.arkkio@aalto.fi).

T. P. Holopainen is with the Department of Technology Development, ABB Motors and Generators, Helsinki, Finland. He was visiting researcher at the Department of Electrical Engineering and Automation, Aalto University School of Electrical Engineering, Espoo, Finland (e-mail: timo.holopainen@fi.abb.com).

iron losses are found to be affected more significantly by the specific loss density increase. Depending on the assumed frequency-dependency of the iron loss, the total increase is 14.1-37.6 %. In addition, the permeability decrease is found to increase the terminal current, which leads to a 4 % increase in the stator resistive losses.

II. Methods

A. Material Identification

In [8], we used a simple 1-D analytical approach for modeling an electrical steel sheet strip with damaged edges (Fig. 1). By assuming uniform material properties at the damaged edge region and applying a curve-fitting procedure to the measurements of [1], we were able to identify the effective width of the edge region as well as the magnetization properties and the specific loss curves for both the intact material and the edge region. Fig. 2 shows the identified magnetization $H(B)$ and loss density $p(B)$ curves, B meaning the flux density, H the magnetic field strength, and p the power loss per unit mass. A value of 1.69 mm was obtained for the width of the edge region, which is in agreement with the conclusion in [5], that the whole 3 mm tooth is affected by cutting.

The iron losses are known to consist of hysteresis (subscript hy), classical eddy-current (cl) and excess (ex) loss components. In a lamination excited by a sinusoidal flux density with an amplitude B and frequency f, these three components can usually be approximated as

$$p_{\mathrm{hy}} = c_{\mathrm{hy}} f B^{1.6\ldots2} \tag{1a}$$

$$p_{\mathrm{cl}} = c_{\mathrm{cl}} \left(fB\right)^2 \tag{1b}$$

$$p_{\mathrm{ex}} = c_{\mathrm{ex}} \left(fB\right)^{1.5}, \tag{1c}$$

where c_{hy}, c_{cl} and c_{ex} are constant parameters. However, since the measurements in [1] were done only at 50 Hz, we don't have any information of the frequency dependency of the core losses and the three loss components cannot be separated. Thus quadratic polynomials cB^2 were fitted to the 50 Hz $p(B)$ curves of Fig. 2 (b) in order to obtain loss coefficients c specific to the 50 Hz excitation for both the intact material and the edge region. In the induction motor simulations, we then consider two cases in which the iron loss of Fig. 2 (b) comprises either only the hysteresis loss or only the eddy-current loss, meaning that

$$\text{either} \quad \begin{cases} c_{\mathrm{hy}} = \dfrac{c}{50\ \mathrm{Hz}} \\ c_{\mathrm{cl}} = c_{\mathrm{ex}} = 0 \end{cases} \quad \text{or} \quad \begin{cases} c_{\mathrm{hy}} = c_{\mathrm{ex}} = 0 \\ c_{\mathrm{cl}} = \dfrac{c}{\left(50\ \mathrm{Hz}\right)^2} \end{cases}. \tag{2}$$

The eddy-current losses depend mostly on the thickness and electrical conductivity of the sheets, and thus should not be very much affected by the cutting. However, the excess losses can be significantly affected by plastic deformation which occurs in the cutting process [9]. Here we assume that the excess losses are included in the eddy-current loss expression (1b), and thus expect (2) to give the maximum and minimum frequency dependencies of the iron loss for the material measured in [1]. The actual frequency dependency of the losses is expected to fall somewhere between these two extreme cases.

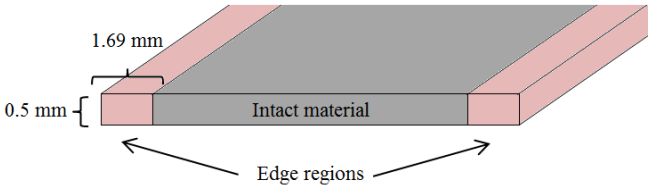

Fig. 1. Illustration of the edge regions and intact material at the end of a 0.5 mm thick steel-sheet strip.

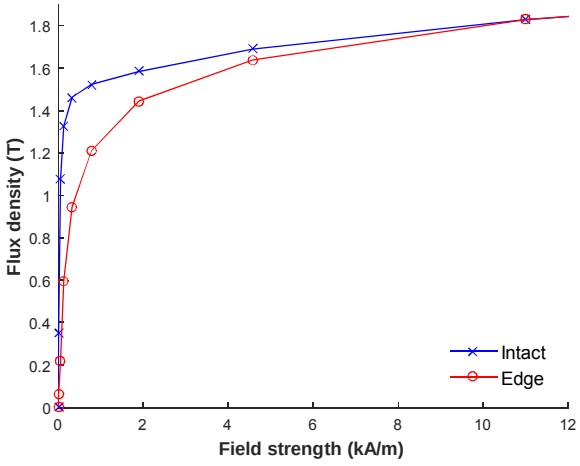

(a)

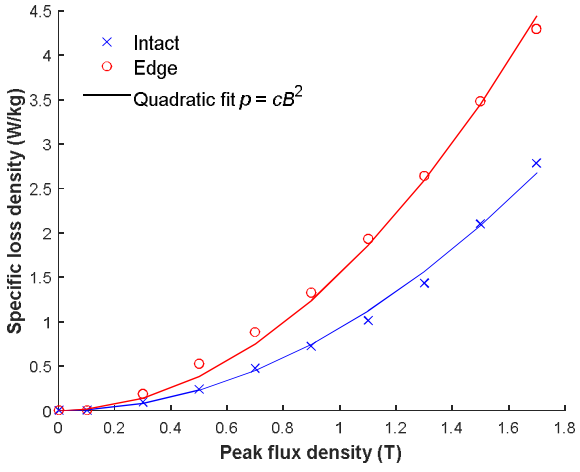

(b)

Fig. 2. (a) Magnetization and (b) specific loss curves identified for the intact and edge regions of electrical steel-sheet samples [8]. Quadratic polynomials have been fitted to the loss curves for the FE computation.

B. Finite-Element Model of Induction Machine

A 37 kW 4-pole induction motor is studied. The rated data and some dimensions of the machine are shown in Table I. The machine is simulated with the 2-D FE method described in details in [10]. One quarter of the cross-sectional (x-y) plane of the machine is considered. The FE mesh in Fig. 3 shows the finely discretized edge region around the laminated core. The mesh consists of 14470 linear elements and 7644 nodes.

The flux density is expressed as the curl of a magnetic vector potential whose nodal values are included in vector $\boldsymbol{a}$. The Ampere's law is expressed weakly using the Galerkin method. The stator winding is supplied from a voltage source, and the stator currents $\boldsymbol{i}$ are solved together with the field equations. The spatially discretized equation system to be solved is

$$\boldsymbol{S}(\boldsymbol{a})\boldsymbol{a} + \boldsymbol{T}\frac{d\boldsymbol{a}}{dt} + \boldsymbol{D}\boldsymbol{i} = \boldsymbol{0} \tag{3}$$

$$n_{\mathrm{sym}} l \boldsymbol{D}^{\mathrm{T}} \frac{d\boldsymbol{a}}{dt} + \boldsymbol{R}\boldsymbol{i} + \boldsymbol{L}\frac{d\boldsymbol{i}}{dt} = \boldsymbol{u}\,, \tag{4}$$

in which $\boldsymbol{S}$ and $\boldsymbol{T}$ are the stiffness and damping matrices, $\boldsymbol{D}$ is a matrix which determines the stator winding flux-linkages, $n_{\mathrm{sym}} = 4$ is the number of symmetry sectors, l is the axial length of the machine, matrices $\boldsymbol{R}$ and $\boldsymbol{L}$ include the stator resistances and end-winding inductances, and $\boldsymbol{u}$ the voltages applied to the stator winding. Matrix $\boldsymbol{S}$ depends on $\boldsymbol{a}$ due to the nonlinear magnetization properties in the laminated core (Fig. 2 (a)). Matrix $\boldsymbol{T}$ is nonzero only in the rotor bars and the shaft, which have a nonzero electrical conductivity. The ordinary differential equations (3) and (4) are integrated in time using the backward-Euler method and the rotor of the machine is rotated with a constant speed using the moving-band technique.

After the field solution, the iron losses are calculated in the post-processing from the Fourier series decomposition of the magnetic flux density vector $\boldsymbol{B}(x,y,t)$. The iron-loss density is summed for each harmonic separately as

$$p(x,y) = \sum_i \left(c_{\mathrm{hy}} + c_{\mathrm{cl}} f_i\right) f_i \left|\boldsymbol{B}_i(x,y)\right|^2 \tag{5}$$

in which only either c_{hy} or c_{cl} is nonzero according to (2). The total losses are obtained by integrating (5) over the volume of the machine. It is not theoretically correct to superpose the losses for each harmonic, and we usually prefer more accurate time-domain loss models. However, (5) can be implemented even with the limited amount of information in the single-frequency $p(B)$ curve of Fig. 2 (b), and is expected to give a rough estimate of the loss mechanisms due to the cutting.

III. Application and Results

A. Iron-Loss Mechanisms

In the motor, the cutting affects the losses in two distinct ways. First of all, the reduced permeability at the edges (Fig. 2 (a)) forces the flux deeper into the iron core which increases the flux density and thus the losses. On the other hand, the cutting also has a direct effect on the specific loss density curves (Fig. 2 (b)). The total loss increase in the machine is a combination of these two effects, which cannot be distinguished by measurements. However, with simulation we can study in which proportion these two mechanisms influence the losses. We thus apply the FE method to perform the following case studies:

- Case 1: Undamaged core, where the edge region is modeled with the intact $H(B)$ and $p(B)$ curves.
- Case 2: Damaged core, where the edge region is modeled with the deteriorated $H(B)$ curve and the intact $p(B)$ curve.
- Case 3: Damaged core, where the edge region is modeled with the deteriorated $p(B)$ curve and the intact $H(B)$ curve.
- Case 4: Damaged core, where the edge region is modeled with the deteriorated $H(B)$ and $p(B)$ curves.

TABLE I
Rated Data and Some Dimensions of the Motor

Shaft power	37 kW
Voltage	400 V
Frequency	50 Hz
Connection	Star
Number of pole pairs	2
Stator outer diameter	310 mm
Stator inner diameter	200 mm
Air gap	0.8 mm
Number of stator slots	48
Number of rotor slots	40

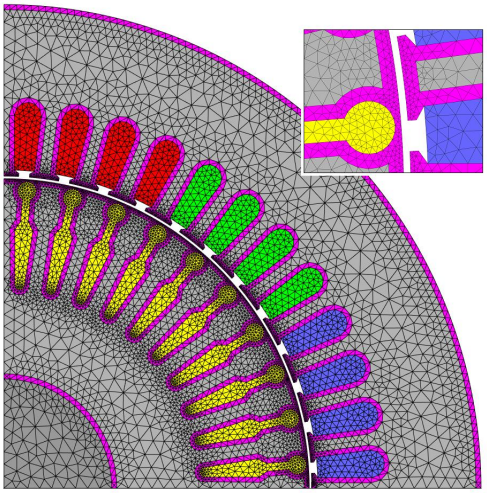

Fig. 3. FE mesh of the studied 37 kW induction motor. The 1.69-mm edge regions around the laminated core are shown in purple color.

Each of the above cases is simulated twice so that either only the hysteresis or eddy-current losses are considered according to (2) and (5). The FE mesh is the same for each case to eliminate the effect of discretization errors on the results.

B. Simulation Results

Each of the above four cases is simulated by forcing the rotor to rotate with the slip that gives the rated shaft power in Case 1. The stator winding is supplied by the rated sinusoidal terminal voltages. 500 time steps are used per one supply period in the time-stepping FE simulation. An initial state is calculated with a time-harmonic solution, and the machine is simulated for three supply periods. The results are averaged over the last period.

Fig. 4 compares the instantaneous rated-load flux-density distributions in Cases 1 and 2 to study the effect of the reduced permeability at the edges. It is clear from the results of Case 2 that the reduced permeability forces the flux density away from the edges. From the difference plot it is seen that the flux densities increase slightly in the teeth through which the flux lines pass to the air gap. However, clearly the largest differences are seen in the teeth in the middle part of the studied quarter. This means that the deterioration actually forces the flux to divide more equally between the teeth. In Case 1 the flux mainly passes through the three leftmost stator and rotor teeth, while in Case 2 the flux passes through the four or five leftmost teeth. Thus the effect of the permeability decrease on the iron loss may actually be smaller than what we initially expected.

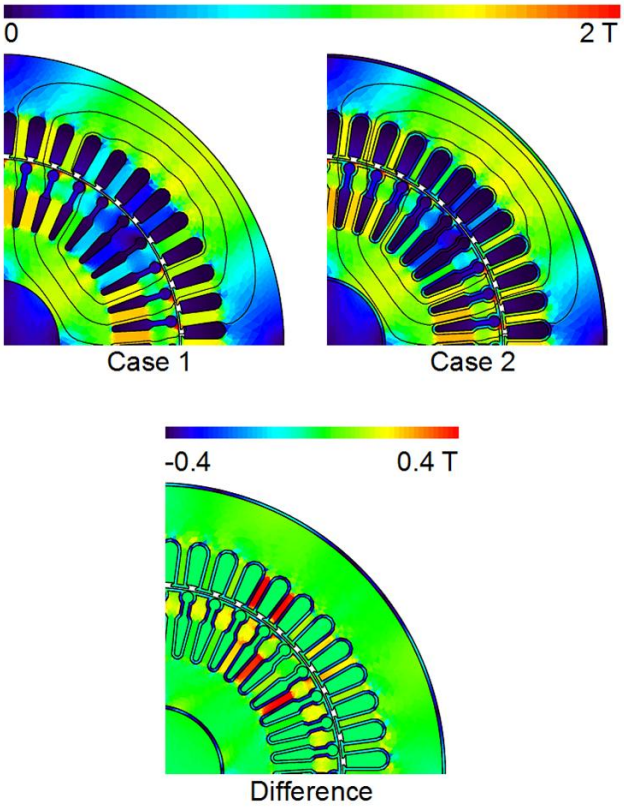

Fig. 4. Flux-density distributions in Case 1 and Case 2, and the difference between these two.

Table II shows the iron losses calculated in the four studied cases and when either the hysteresis or the eddy-current losses are considered in the laminated core. Also the difference of the other cases to Case 1 is shown. Indeed, the difference in the total iron loss between Cases 1 and 2 is less than 3.3 %, which means that the decreased permeability affects the losses rather little. The difference between Cases 1 and 3 shows that the direct effect on the specific loss is 14.8-36.9 %, and thus much more significant. The combined effect in Case 4 is about the same, 14.1-37.6 %, which is in agreement with the recent results in [11].

In both the stator and the rotor, the cutting mostly affects the eddy-current loss. The rotor hysteresis loss is almost negligible due to the fact that the rotor losses are mostly caused by high-frequency flux-density harmonics. This is also seen in the loss-density distributions in Fig. 5. The maximum eddy-current loss densities are much higher than the maximum hysteresis-loss densities, but they occur on a very small region close to the air gap, where the flux density has high-frequency harmonics.

In rotating electrical machines, the performance is mainly determined by the air gap, and the magnetic properties of the core have less influence on the operating characteristics than, for example, in transformers and inductors. Indeed, the operating point of the motor is very little affected by the permeability reduction. The electrical active power, torque and shaft power change less than 0.3 % when changing from Case 1 to Case 2. However, the power factor decreases by 1.7 %, and the rms terminal current increases by 2.0 %, which increases also the stator resistive losses by 4.0 %. This increase is actually higher than the increase in the iron loss due to the permeability reduction and very well in agreement with the estimation of [4].

TABLE II
IRON LOSS AT THE RATED LOAD IN THE FOUR STUDIED CASES WHEN EITHER HYSTERESIS OR EDDY-CURRENT LOSSES ARE CONSIDERED AND DIFFERENCES COMPARED TO CASE 1

Location	Loss	Case 1	Case 2	Case 3	Case 4
Stator	hy	147 W	153 W	168 W	167 W
	cl	293 W	306 W	371 W	387 W
Rotor	hy	3.2 W	3.1 W	4.9 W	4.8 W
	cl	178 W	167 W	273 W	260 W
Total	hy	151 W	156 W	173 W	172 W
	cl	471 W	473 W	644 W	647 W
Stator	hy	-	+3.5 %	+14.0 %	+13.4 %
	cl	-	+4.4 %	+26.6 %	+32.2 %
Rotor	hy	-	-3.7 %	+53.1 %	+47.5 %
	cl	-	-5.8 %	+54.0 %	+46.5 %
Total	hy	-	+3.3 %	+14.8 %	+14.1 %
	cl	-	+0.6 %	+36.9 %	+37.6 %

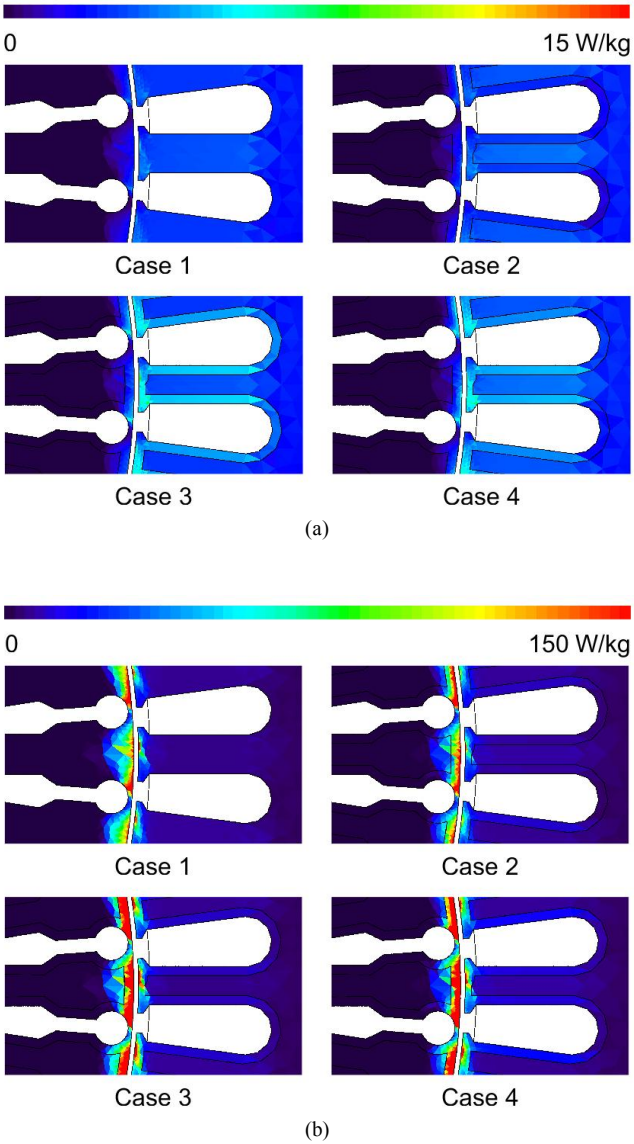

Fig. 5. Iron-loss distributions close to the air gap in the four studied cases when (a) only hysteresis losses and (b) only eddy-current losses are considered.

The total electromagnetic loss increase between Cases 4 and 1 is 11.7 % if the hysteresis losses are considered and 29.6 % if the eddy-current losses are considered. With more realistic iron-loss coefficient, the loss increase should lie somewhere between these limits.

IV. Discussion and Conclusions

The iron losses in a 37 kW induction machine were studied by numerical simulations by taking into account the deteriorated magnetization properties and increased power-loss densities around the cutting edges of the core laminations. The material properties were modeled based on the work presented in [1] and [8].

The obtained 1.69 mm width for the damaged edge layer should not be seen as a unique solution for the identification problem presented in [8]. It is likely that the model identification could also lead to a smaller width and more deteriorated material properties, or vice versa. Our ongoing research aims for addressing the effect of the identification results on the estimated induction machine losses, as well as separation of the hysteresis, eddy current and excess losses from measurements at several frequencies. In addition to the damaged magnetization properties, additional eddy current losses are likely to arise due to the punching which deteriorates the insulation and causes galvanic contacts between adjacent core laminations. These losses have been studied in [12].

According to the simulation results based on a single machine, the cutting increases the iron loss mainly due to the direct influence on the specific loss density curve, and the effect of the reduced permeability on the edges is rather small. This is in agreement with the findings of [13], in which the effect of shrink fitting on the hysteresis losses of a permanent-magnet machine was studied. Intuitively, we were expecting the permeability decrease alone to have a larger influence on the losses, since the deteriorated edge region covers 49.3 % of the stator tooth width. However, in the studied motor, considering the deteriorated permeability at the edges lead to a more even distribution of the flux between the stator teeth. Thus the flux density and the losses in the teeth didn't increase as much as we originally expected. This also implies that designing a machine with wider teeth as an attempt to compensate for the damage at the edge may not significantly reduce the losses. However, the effect might be different in a salient-pole machine where the flux mainly passes through the teeth close to the pole surface.

Since the machine was supplied from a voltage source, reduction of the permeability also increased the required magneto-motive force which resulted in a larger terminal current. This caused the resistive losses to increase by 4.0 %. The increase in the total electromagnetic losses due to the cutting was found to be 11.7-29.6 %. This is a rather significant increase which should be taken into account in the thermal design of machines which are not annealed after assembling the cores.

Finally, the results in [1] were obtained for a rather low-loss electrical steel material, whose power-loss density at 1 T and 50 Hz excitation is less than 1 W/kg. Knowing that the authors of [1] represent the steel industry, it is likely that the used materials and the cutting tools were of very high quality. In practice, the cutting tool wears in use which increases the damage caused to the sheets. The effect of the cutting on the iron loss is a stochastic phenomenon and accurate prediction of the losses in a single electrical machine can be rather challenging. However, the rough agreement of the experimental and numerical results presented in [5]-[7], [11], [13], and here gives evidence on how much the losses of electrical machines are affected by the cutting and other kind of processing.

V. Acknowledgment

T. P. Holopainen gratefully acknowledges the opportunity to work as visiting researcher at the Department of Electrical Engineering and Automation, Aalto University School of Electrical Engineering.

VI. References

[1] A. Schoppa, J. Schneider, and J.-O. Roth, "Influence of the cutting process on the magnetic properties of non-oriented electrical steels," *J. Magn. Magn. Mater.*, Vol. 215-216, pp. 100-102, 2000.

[2] M. Emura, F. J. G. Landgraf, W. Ross, and J. R. Barreta, "The influence of cutting technique on the magnetic properties of electrical steels," *J. Magn. Magn. Mater,* Vol. 254-255, pp. 358-360, 2003.

[3] R. Siebert, J. Schneider, E. Beyer, "Laser Cutting and Mechanical Cutting of Electrical Steels and Its Effect on the Magnetic Properties," *IEEE Trans. Magn.*, Vol. 50, No. 4, Art. no. 2001904, Apr. 2014.

[4] M. Bali, A. Muetze, "Influences of CO_2 Laser, FKL Laser, and Mechanical Cutting on the Magnetic Properties of Electrical Steel Sheets," *IEEE Trans. Ind. Appl.*, Vol. 51, No. 6, pp. 4446-4454, Nov./Dec. 2015.

[5] F. Ossart, E. Hug, O. Hubert, C. Buvat, and R. Billardon, "Effect of punching on electrical steels: experimental and numerical coupled analysis," *IEEE Trans. Magn.*, Vol. 36, No. 5, pp. 3137-3140, Sep. 2000.

[6] M. Bali, H. De Gersem, A. Muetze, "Finite-Element Modeling of Magnetic Material Degradation Due to Punching," *IEEE Trans. Magn.*, Vol. 50, No. 2, Art. no. 7018404, Feb. 2014.

[7] K. Fujisaki, R. Hirayama, T. Kawachi, S. Satou, C. Kaidou, M. Yabumoto, and T. Kubota, "Motor core iron loss analysis evaluating shrink fitting and stamping by finite-element method," *IEEE Trans. Magnetics*, Vol. 43, No. 5, pp. 1950-1954, May 2007.

[8] T. P. Holopainen, P. Rasilo, A. Arkkio, "Identification of Magnetic Properties for Cutting Edge of Electrical Steel Sheets," under review for ICEM, Lausanne, Switzerland, September 2016.

[9] V. Permiakov, L. Dupré, A. Pulnikov, J. Melkebeek, "Loss separation and parameters for hysteresis modelling under compressive and tensile stresses," *J. Magn. Magn. Mater.*, Vol. 272-276, pp. 553-554, January, 2004.

[10] A. Arkkio, "Analysis of Induction Motors Based on the Numerical Solution of the Magnetic Field and Circuit Equations," Ph.D. thesis, Helsinki University of Technology, 1987. Available at http://lib.tkk.fi/Diss/198X/isbn951226076X/.

[11] M. Bali, H. De Gersem, A. Muetze, "Determination of Original Non-Degraded and Fully Degraded Magnetic Properties of Material Subjected to Mechanical Cutting," *IEEE Trans. Ind. Appl.*, in press, 2016.

[12] S. Bikram Shah, P. Rasilo, A. Belahcen, A. Arkkio, "Estimation of Additional Losses due to Random Contacts at the Edges of Stator of an Electrical Machines," *COMPEL*, Vol. 34, No. 5, pp. 1501-1510, 2015.

[13] P. Rasilo, U. Aydin, D. Singh, F. Martin, R. Kouhia, A. Belahcen, A. Arkkio, "Multiaxial Magneto-Mechanical Modeling of Electrical Machines with Hysteresis," to be presented at *PEMD*, Glasgow, United Kingdom, April 2016.

VII. Biographies

Paavo Rasilo received his M.Sc. (Tech.) and D.Sc. (Tech.) degrees from Helsinki University of Technology (currently Aalto University) and Aalto University, Espoo, Finland in 2008 and 2012, respectively. He is currently working as an Assistant Professor at the Department of Electrical Engineering, Tampere University of Technology, Tampere, Finland. His research interests deal with numerical modeling of electrical machines as well as power losses and magnetomechanical effects in soft magnetic materials.

Ugur Aydin received his M.Sc. degree from Vilnius Gediminas Technical University, Electrical Energetics Systems Engineering, Vilnius, Lithuania in 2012. He is currently working towards the Ph.D. degree at the Department of Electrical Engineering and Automation, Aalto University Espoo, Finland. His research focuses on magnetomechanical effects on soft magnetic materials and losses in electrical machines.

Timo Holopainen received his M.Sc. degree in 1987 from Helsinki University of Technology, Mechanical Engineering. He began his career at VTT Manufacturing Technology working with strength and vibration control of marine structures. Later, he focused on vibrations of rotating machines and received his Dr. Tech. degree from Helsinki University of Technology, Electrical Engineering. Currently he works with rotordynamics and vibration control of large electric motors at ABB Motors and Generators, Technology Development. He is a member of API 684 Task Force (Rotordynamic Tutorial) and IFToMM Technical Committee for Rotordynamics.

Antero Arkkio was born in Vehkalahti, Finland in 1955. He received his M.Sc. (Tech.) and D.Sc. (Tech.) degrees from Helsinki University of Technology in 1980 and 1988. Currently he is a Professor of Electrical Engineering at Aalto University. His research interests deal with modeling, design, and measurement of electrical machines.